



Published in final edited form as:

Life Sci. 2015 February 15; 123: 61–71. doi:10.1016/j.lfs.2014.12.024.

Heart failure duration progressively modulates the arrhythmia substrate through structural and electrical remodeling

Victor P. Long III^{1,2}, Ingrid M. Bonilla^{1,2}, Pedro Vargas-Pinto³, Yoshinori Nishijima¹, Arun Sridhar¹, Chun Li¹, Kent Mowrey⁵, Patrick Wright⁴, Murugesan Velayutham², Sanjay Kumar¹, Nam Lee^{1,2}, Jay L Zweier^{2,4}, Peter J. Mohler^{2,4}, Sandor Györke^{2,4}, and Cynthia A. Carnes^{1,2,4}

¹College of Pharmacy, The Ohio State University, Columbus, OH, USA

²Dorothy M. Davis Heart and Lung Research Institute, The Ohio State University, Columbus, OH, USA

³College of Veterinary Medicine, The Ohio State University, Columbus, OH, USA

⁴Department of Physiology and Cell Biology, The Ohio State University, Columbus, OH, USA

⁵St Jude Medical, Sylmar CA, USA

Abstract

AIMS—Ventricular arrhythmias are a common cause of death in patients with heart failure (HF). Structural and electrical abnormalities in the heart provide a substrate for such arrhythmias. Canine tachypacing-induced HF models of 4–6 weeks duration are often used to study pathophysiology and therapies for HF. We hypothesized that a chronic canine model of HF would result in greater electrical and structural remodeling than a short term model, leading to a more arrhythmogenic substrate.

MAIN METHODS—HF was induced by ventricular tachypacing for one (short-term) or four (chronic) months to study remodeling.

KEY FINDINGS—Left ventricular contractility was progressively reduced, while ventricular hypertrophy and interstitial fibrosis were evident at 4 month but not 1 month of HF. Left ventricular myocyte action potentials were prolonged after 4 (p<0.05) but not 1 month of HF. Repolarization instability and early afterdepolarizations were evident only after 4 months of HF

Address for correspondence: Cynthia Carnes PharmD, PhD, College of Pharmacy, 500 W 12th Ave, Columbus, OH 43210. Fax: 614-292-1335; Tele: 614-292-1715; carnes.4@osu.edu.

M. Velayutham: Department of Cardiothoracic Surgery, University of Pittsburgh Medical Center, Pittsburgh, PA 15219, USA

A. Sridhar: GSK Bioelectronics R&D, Gunnels Wood Road, Stevenage SG1 2NY, Hertfordshire, UK

P. Vargas-Pinto: Universidad de la Salle. Bogotá, Colombia

Y. Nishijima: MCW Cardiovascular Center, Medical College of Wisconsin, 8701 Watertown Plank Rd, Milwaukee, WI 53226

C Li: Department of Cardiovascular Medicine, Peking University People's Hospital

Publisher's Disclaimer: This is a PDF file of an unedited manuscript that has been accepted for publication. As a service to our customers we are providing this early version of the manuscript. The manuscript will undergo copyediting, typesetting, and review of the resulting proof before it is published in its final citable form. Please note that during the production process errors may be discovered which could affect the content, and all legal disclaimers that apply to the journal pertain.

Disclosures:

None

($p < 0.05$), coinciding with a prolonged QTc interval ($p < 0.05$). The transient outward potassium current was reduced in both HF groups ($p < 0.05$). The outward component of the inward rectifier potassium current was reduced only in the 4 month HF group ($p < 0.05$). The delayed rectifier potassium currents were reduced in 4 ($p < 0.05$) but not 1 month of HF. Reactive oxygen species were increased at both 1 and 4 months of HF ($p < 0.05$).

SIGNIFICANCE—Reduced I_{to} , outward I_{K1} , I_{Ks} , and I_{Kr} in HF contribute to EAD formation. Chronic, but not short term canine HF, results in the altered electrophysiology and repolarization instability characteristic of end-stage human HF.

Keywords

heart failure; electrophysiology; fibrosis; hypertrophy

Introduction

Heart failure (HF) is a leading contributor to morbidity and mortality. In 2010, the number of deaths in the US attributed to HF was ~279,000, and HF was noted in 1 of 9 death certificates (Go et al. 2014). Sudden death due to lethal ventricular arrhythmias is six- to ninefold higher in HF patients than in the general population (Tomaselli and Zipes 2004; Thom et al. 2006), and accounts for up to 50% of deaths in HF patients (Tomaselli and Zipes 2004).

HF is associated with both structural and electrical remodeling that transforms the normal myocardium into a substrate susceptible to arrhythmogenesis. Left ventricular dilation, hypertrophy, and fibrosis are all examples of compensatory changes that are initially adaptive in the failing heart (Cohn et al. 2000). These changes may progress to become maladaptive resulting in further deterioration of heart function, and have been linked to the development of arrhythmia and/or sudden death (Hsia and Marchlinski 2002; Iles et al. 2011; Haider et al. 1998). At the cellular level, cardiomyocytes of the failing heart display electrical remodeling, including a signature prolongation of the action potential (AP) (Beuckelmann et al. 1995; Akar and Rosenbaum 2003).

We previously reported that chronic (four or more months) canine tachypacing HF becomes irreversible and emulates multiple aspects of chronic human HF (Nishijima et al. 2005). In the present study, we tested the hypothesis that dogs paced into chronic HF (4 M HF) would demonstrate greater structural and electrophysiological remodeling than dogs paced into acute HF (1 M HF), providing a substrate for ventricular arrhythmias. We used serial echocardiography and electrocardiograms to assess ventricular function and electrical activity, respectively. Patch clamp recordings were used to measure action potentials and K^+ currents in ventricular myocytes. Real-time polymerase chain reaction (RT-PCR) was used to quantify ion channel subunit mRNA.

Materials and Methods

Heart failure canine model

All animal procedures were approved by the Institutional Animal Care and Use Committee of the Ohio State University. A total of 63 adult mixed breed dogs of either sex (2–5 years of age) weighing between 8 and 20 kg with normal cardiac function were used. Dogs were verified to have normal cardiac function by routine electrocardiograms and echocardiographic examinations during butorphanol tartrate (0.5 mg kg^{-1} intramuscularly) sedation. Dogs had a RV pacemaker lead implanted in the RV apex, and HF was induced ($n=16$) by tachypacing for four months as previously described (Sridhar et al. 2009). To assess time dependence during the progression of HF, echocardiograms and electrocardiogram were measured at baseline, after 1 month, and 4 months of pacing in the 4 M HF group. A second group of dogs was RV tachypaced for 1 month at 180 bpm ($n=17$) and echocardiograms were measured at baseline and at the end of the pacing protocol as previously reported. (Nishijima et al. 2007; Nishijima et al. 2005). An age matched group of 30 healthy dogs were used as controls and studied in parallel. Transmural samples of left ventricular tissue were formalin fixed and embedded in paraffin and sectioned to $5 \mu\text{m}$ thickness, using standard procedures. Tissue sections were stained with Masson's Trichrome to define the percentage area of fibrosis, as previously described (Nishijima et al. 2007)

Myocyte Isolation

On the day of the terminal procedure, the dogs were anesthetized with pentobarbital sodium (50 mg/kg IV). The heart was rapidly removed and perfused with cold cardioplegia solution containing the following in mM: NaCl 110, CaCl_2 1.2, KCl 16, MgCl_2 16 and NaHCO_3 10. Cannulation of the left circumflex artery was used to perfuse the left ventricle, as previously described. (Sridhar et al. 2009; Bonilla et al. 2013a) Adjacent tissue samples were collected and snap frozen for protein analyses. Tyrode's solution (mM) containing NaCl 130, KCl 5.4, MgCl_2 3.5, NaH_2PO_4 0.5, Glucose 10, HEPES 5 and taurine 20, was used as the initial perfusate. During the cell isolation process the heart was perfused with three different solutions (36°C). First the heart was perfused for 10 minutes with Tyrode's solution with 0.1 mM EGTA; followed by perfusion with Tyrode's solution containing 0.3 mM Calcium, 0.12 mg/ml of Trypsin Inhibitor (NIBCO) and 1.33mg/ml of collagenase (Type II, Worthington), for a maximum of 45 minutes. Following enzymatic digestion, the heart was perfused with normal Tyrode's solution for five minutes to remove residual enzyme. After digestion, the cells were resuspended in incubation buffer. This isolation procedure typically yields 40–60% rod shaped ventricular myocytes. All myocyte electrophysiology experiments were conducted within 10 hours of isolation.

Electrophysiological recordings

To assess myocyte electrophysiology, Amphotericin-B perforated patch clamp techniques with a bath temperature of $36 \pm 0.5^\circ\text{C}$ were used. The myocytes were placed in a laminin coated cell chamber (Cell Microcontrols, Norfolk, VA) and superfused with bath solution containing (in mM): 135 NaCl, 5 MgCl_2 , 5 KCl, 10 glucose, 1.8 CaCl_2 , and 5 HEPES with pH adjusted to 7.40 with NaOH. For current measurements the calcium in the bath solution was reduced to 1.0mM in addition, $2 \mu\text{M}$ nifedipine was added to the bath solution to avoid

contamination with L-type Ca^{2+} current. Borosilicate glass micropipettes with tip resistance of 1.5–4.5 $\text{M}\Omega$, were filled with pipette solution containing the following (in mM): 100 K-aspartate, 40 KCl, 5 MgCl, 5 EGTA, 5 HEPES, pH adjusted to 7.2 with KOH.

Action potentials (AP) were recorded in a train of 25 traces at 0.5, 1 and 2 Hz. The average of the last 10 traces (i.e. from trace 16–25) was used to calculate the action potential duration (APD). APD was calculated at 50 and 90 percent of repolarization (APD₅₀ and APD₉₀). The standard deviation of the APD₉₀ for the last 10 traces not exhibiting EADs was used to evaluate repolarization variability (Thomsen et al. 2004). EADs were defined as positive oscillations occurring in Phase 2 or Phase 3 of the APD.

For current recordings, only recordings with an access resistance $<20 \text{ M}\Omega$ were included in the analyses. Transient outward potassium current (I_{to}), potassium inward rectifying current (I_{K1}), and delayed rectifying currents ($I_{\text{Kr}} + I_{\text{Ks}}$) were elicited as previously described. (Sridhar et al. 2008; Bonilla et al. 2013b) To assess steady state inactivation kinetics of I_{to} , a series of 500 ms prepulses were clamped to voltages between -80 mV and $+10 \text{ mV}$ (holding potential of -60 mV) followed by a 300 ms step to $+50 \text{ mV}$ (peak current) (Nabauer et al. 1993). I_{to} elicited during each prepulse was normalized to peak current and plotted against the respective prepulse potential. The AUC for the window current was defined as the area beneath the intersection of the normalized I_{to} activation and inactivation curves, in the voltage range between -50 to $+10 \text{ mV}$. To investigate I_{to} recovery from inactivation, a two-step protocol was used in which two 200 ms pulses from a holding potential of -60 mV to $+40 \text{ mV}$ were separated by a variable interpulse interval of 20 to 1000 ms (Nabauer et al. 1993). Rectification ratio was calculated as previously described (Carnes and Dech 2002; Lopatin et al. 2000).

Data was collected with a low noise data acquisition system Digidata 1440A (Molecular devices, Sunnyvale, CA), Clampex software and an Axopatch 200A amplifier (Axon Instruments, Sunnyvale, CA).

Immunoblots

Following protein quantification, tissue lysates were analyzed on Mini-PROTEAN tetra cell (BioRad) on a 4–15% precast TGX gel (BioRad) in Tris/Glycine/SDS Buffer (BioRad). Gels were transferred to a nitrocellulose membrane using the Mini-PROTEAN tetra cell (BioRad) in Tris/Glycine buffer with 20% methanol (v/v, BioRad). Membranes were blocked for 1 hour at room temperature using a 3% BSA solution and incubated with primary antibody overnight at 4°C . Antibodies were KChiP2 (Alomone, Santa Cruz), Kv4.3 (Covance), and GAPDH (Fitzgerald). Donkey anti-rabbit-HRP (Jackson Laboratories) was used as the secondary antibody. Densitometry was performed using Image lab software and all data was normalized to GAPDH levels present in each sample.

Real-time PCR for gene expression

Total RNA was extracted from the cardiac tissues with Trizol reagent (Invitrogen), and $2 \mu\text{g}$ RNA was then converted to cDNA by using the High Capacity cDNA Reverse Transcription Kit (Applied Biosystems). Gene expression was quantified by real-time RT-PCR (Light Cycler 96, Roche Applied Science) using SYBR green assay reagent and gene-specific

primer listed in Table 1. Relative amplification was quantified by normalizing the gene-specific amplification to that of 18s rRNA in each sample. Changes in mRNA abundance were calculated using 2^{-C_T} method (Livak and Schmittgen 2001; Kumar et al. 2013). qPCR reactions were run in triplicates. Primers used were as follows (5'-3'):

Kv11.1 (forward: CCTGCTGCTGGTCATCTACA; reverse: TCCTCGTTGGCATTGACATA), KCNE2 (forward: GAACACGACAGCTGAGCAAG; reverse: ACTGGTGGTAGGGGTCATTG), KChiP2 (forward: GCTGGTTTGTCCGGTGATTCT; reverse: AAGAAGCTCTCCACGTGCTC), KCNQ1 (forward: CTTTACCTGCCAGGGGTACA; reverse: ACCACATACTCCGTCCCAAA), DPP6 (forward: CCCATCGAGTGTCCAGCACTA; reverse: GATGGATCGGTACAGGTGCT), Kv4.3 (forward: GTTTGAGCAGAACTGCATGG; reverse: GTGGATGGTGTGAGCTCTT), KCNJ2 (forward: TATCAACGTTGGGTTTCGACA; reverse: AAATCAGTTATGGTTCCTTTGGT); 18s (forward: GCTCTAGAATTACCACAGTTATC; reverse: AAATCAGTTATGGTTCCTTTGGT)

Electron paramagnetic resonance (EPR) spectroscopy

The ventricular tissue samples were flash frozen and stored in liquid nitrogen prior to electron paramagnetic resonance (EPR) analysis to measure radical and paramagnetic species. Both semi-quinone radical and Fe-S centers were quantified using previously described methods (Nishijima et al. 2011; Zweier et al. 1989; Zweier et al. 1987). Each EPR sample was prepared by transferring the frozen heart tissue (235–570 mg) into a ceramic mortar pre-chilled with liquid nitrogen. The tissue was then crushed in liquid nitrogen using a pestle. The tissue in liquid N₂ was then loaded into a finger Dewar containing liquid nitrogen. Low temperature, 77 K, EPR spectra were recorded with a Bruker ESP 300E spectrometer (Bruker BioSciences, Billerica, MA, USA) operating at X-band with 100 KHz modulation frequency and a TM₁₁₀ cavity as described previously (Zweier et al. 1995). The finger Dewar containing heart tissue samples in liquid nitrogen was placed within the EPR spectrometer cavity. All spectra were recorded with the following parameters: receiver gain = 1×10^5 , modulation amplitude = 2 G (4 G for Fe-S signals), time constant = 164 ms, scan time = 60 s, microwave power = 1 mW (20 mW for Fe-S signals), and number of scans = 10.

Data Analysis

Cellular electrophysiology data were analyzed using Clampfit 10.3 software (Axon Instruments) and Origin 9.0 software (OriginLab, Northampton, MA, USA). One way repeated measured ANOVA was used to analyze differences within groups, while comparison between groups was analyzed by one-way ANOVA with post hoc least significant difference testing or Student's t-test (OriginPro 8.6, OriginLab). Normality was tested via Kolmogorov-Smirnov. Non parametric analysis was performed using Chi-Square. All data are presented as mean \pm SE (or SD for PCR quantification) and $p < 0.05$ was the criterion for statistical significance for all comparisons.

Chemicals

All chemicals used were purchased from Sigma-Aldrich (St. Louis, MO, USA) and Fisher Scientific (Pittsburgh, PA, USA), unless otherwise noted. All buffers and solutions were prepared daily.

Results

Chronic tachypacing is accompanied by an increase in left ventricular mass, a prolonged QTc interval, and interstitial fibrosis

RV tachypacing resulted in significantly impaired contractility, LV chamber dilation and increased LV mass at 4 M HF compared to 1 month HF and baseline (TABLE 1). The corrected QT interval was significantly prolonged at 4 M HF versus baseline.

Ventricular tissue samples (control, 1 M HF, and 4 M HF) had significantly increased fibrosis in the 4 M HF group ($p < 0.05$ vs control) (Figure 1). Collectively, these results suggest that time-dependent decreases in cardiac function with continued RV tachypacing are associated with the development of structural remodeling (cardiac hypertrophy and fibrosis) in chronic (4 M) HF.

Chronic tachypacing results in a prolonged AP associated with early afterdepolarizations, increased myocyte size, and downregulation of repolarizing K⁺ currents

Heart failure prolonged ventricular cardiomyocyte action potentials (Figure 2). In addition to AP prolongation, a disappearance of the prominent phase one “notch” occurred with HF. APD₅₀ was significantly prolonged at all rates tested (0.5, 1, and 2 Hz) in both 1 M HF and 4 M HF groups compared with control myocytes ($p < 0.05$) (Figure 2B). APD₉₀ was significantly increased in 4 M HF compared to both baseline and 1 M HF at all rates ($p < 0.05$) (Figure 2C). Rate-adaptation of the APD was maintained in each group ($p < 0.05$). The beat-to-beat variability of APD₉₀, a marker of proarrhythmic potential (Oosterhoff et al. 2007) (Figure 2D) was significantly increased in the 4 M HF group at all rates versus control ($p < 0.05$), and at 1 Hz versus 1 M HF ($p < 0.05$). Consistent with these findings, EADs were significantly more frequent in the 4 M HF group compared to both control and 1 M HF ($p < 0.05$) (Figure 2E). No change in the resting membrane potential was found between the groups. Collectively, this data suggests that HF duration mediates action potential prolongation and the development of a proarrhythmic ventricular substrate.

Membrane capacitance was used as a measure of ventricular cell hypertrophy. Consistent with the LV mass findings, 4 M HF ventricular myocytes had a significantly larger capacitance (239.5 ± 16.6 , $n=23$, $p < 0.05$) compared to controls (159.0 ± 6.6 pF, $n=52$) and 1 M HF (163.7 ± 9.4 pF, $n=29$)

Transient outward current (I_{to}) density and the corresponding slope conductance was significantly decreased in both 1 M and 4 M HF groups ($p < 0.05$ vs Control) (Figure 3B and 3C). Inactivation of I_{to} was best fitted as the sum of two exponentials, a rapidly inactivating $I_{to,fast}$ (τ_1) and a slowly inactivating $I_{to,slow}$ (τ_2). There was no significant difference in either time constant between groups. Mean τ_1 and τ_2 at +50 mV was 18.4 ± 1.9 ms and 87.3

± 21.1 ms, 11.3 ± 0.80 ms and 43.1 ± 10.2 ms, and 15.8 ± 1.5 ms and 68.9 ± 21.5 ms for control (n=23), 1 M HF (n=5), and 4 M HF (n=10), respectively. The rapidly inactivating component comprised $80.6 \pm 2.6\%$ of the decay current in the control group, $73.7 \pm 6.2\%$ in 1 M HF, and $74.8 \pm 7.1\%$ in 4 M HF (p=NS). A plot of the steady state inactivation of I_{to} against current activation revealed no voltage shift in kinetics (Figure 4A). However, there was a decrease in the overall current available (AUC) in both 1 and 4 M HF compared to controls (AUC values were reduced by 97% for 1 M HF and 63% for 4 M HF). This “window” current peaked around -35 mV, representing approximately 5% of peak I_{to} (Figure 4B). The time for I_{to} recovery from activation was assessed using a two-step protocol (Figure 4C). The time for 50% recovery from inactivation was prolonged in the 4 M HF group vs. controls (185.5 ± 16.9 ms vs. 107.0 ± 17.3 ms, $p < 0.05$).

HF-dependent changes in the inward rectifier current, I_{K1} are shown in Figure 5. There were no significant differences in inward slope conductance between groups. Peak I_{K1} outward current was significantly decreased in 4 M HF compared to controls ($p < 0.05$, Figure 5C). The rectification ratio was significantly increased in 4 M HF ($p < 0.05$ vs control, Figure 5D).

HF-induced alterations in the delayed rectifier currents, I_{Kr} and I_{Ks} are shown in Figure 6. I_{Ks} amplitude was significantly decreased in 4 M HF at all test potentials compared to both 1 M HF and controls (Figure 6B), and I_{Ks} slope conductance was decreased in 4 M HF ($p < 0.05$ vs control) (Figure 6C). I_{Kr} was significantly decreased in 4 M HF compared to 1 M HF and control ($p < 0.05$) (Figure 6D).

Protein and mRNA expression of K Channel Subunits does not correlate with function

I_{to} in the canine ventricle is conducted through channel pore-forming subunits Kv4.3 and Kv1.4, with Kv4.3 being the main alpha subunit contributing to the current (Akar et al. 2004a). Kv4.3 can assemble with multiple accessory proteins including K⁺ channel interacting protein 2 (KChIP2) which can modulate Kv4.3 gating and function (Deschenes et al. 2002). Dipeptidyl-aminopeptidase-like protein 6 (DPP6) also coassembles with Kv4.3, and has been shown to alter I_{to} kinetics (Radicke et al. 2005). Biochemical analysis showed no significant difference between protein expression of Kv4.3 and KChIP2 in the control, 1 M HF, and 4 M HF group (Figure 7A and 7B). In contrast, notable HF-dependent changes were observed in transmural gene expression of K⁺ channel subunits (Figure 7C). The mRNA of the Kv4.3 and Kv1.4 subunits demonstrated no change at 1 M HF, but increased gene expression at 4 M HF ($p < 0.05$ vs control and 1 M HF). Similarly the mRNA levels for KChIP2 and DPP6 increased at 4 M HF. KCNJ2 encodes the Kir2.1 channel, the pore-forming subunit of I_{K1} . At 1 M HF, KCNJ2 gene expression was significantly elevated ($p < 0.05$ vs control), and continued to increase at 4 M HF ($p < 0.05$ vs control, $p < 0.05$ vs 1 M HF). I_{Ks} is carried via a complex which includes the pore-forming K_vLTQ1 (KCNQ1) and minK (KCNE1). Both KCNQ1 and KCNE1 mRNA are significantly upregulated at 4 M HF compared to both control ($p < 0.05$) and 1 M HF ($p < 0.05$). I_{Kr} is carried through Kv11.1 channels, and no differences in Kv11.1 mRNA were found between the three groups.

EPR spectroscopy

EPR spectroscopy revealed a modest increase in semiquinone radicals that did not reach significance in left ventricular tissue among either of the HF groups compared to control ($P=NS$) (Figure 8B). However, Fe-S center signals were significantly increased in both 1 M HF and 4 M HF ($p<0.05$ vs control) (Figure 8C).

Discussion

Large animal models of dilated cardiomyopathy are accepted as a surrogate of the pathology of human HF (Houser et al. 2012). In the present study, we found that the 4 month duration of HF overcomes a limitation of the short-term canine tachypacing model - the lack of structural remodeling. We observed an increase in LV mass at 4 M HF (≈ 1.7 fold), coinciding with an increase in myocyte membrane capacitance (≈ 1.5 fold) – both indicators of hypertrophy. These results are consistent with a previous report of increased LV mass after 7 to 10 months of chronic RV pacing (Nishijima et al. 2005). We also report an increase in interstitial fibrosis at 4 M HF. The appearance of increased fibrosis in 4 to 6 week canine HF models varies between studies (Burashnikov et al. 2014; Akar et al. 2004b; Hanna et al. 2004). A key difference between the current model and previous reports is that our chronic pacing rates are not as rapid (180 bpm vs 240 bpm) resulting in a sustained hypertrophic response not seen in more rapid, short-term pacing models. This notion is supported by our previous work, where we observed increases in LV mass after 10 months of pacing, 6 months of which was maintained at 160 bpm (Nishijima et al. 2005). It is well known that hypertrophy induces the structural remodeling of the collagen matrix necessary for fibrosis. (Weber et al. 1988). The lack of fibrosis in rapid pacing models may be responsible for their “reversible” nature.

A hallmark of HF is downregulation of repolarizing K^+ currents and subsequent AP prolongation. The most studied and consistently downregulated K^+ current in both canine HF models and human HF is I_{to} (Akar et al. 2004a; Beuckelmann et al. 1993; Li et al. 2002), and we found reductions in both 1 M HF and 4 M HF groups. The role of I_{to} in early repolarization is evident as the loss of the prominent phase one “notch” during HF. I_{to} may contribute to the prolonged APD₅₀ in both HF groups, as altered I_{to} can alter I_{Ca} (Sah et al. 2002). The role of I_{to} in late repolarization (APD₉₀) is less clear. The peak of the “window current” we observed is in agreement with findings from other groups (Virag et al., 2011), and suggests I_{to} may contribute repolarizing current during the plateau of the AP.

The molecular mechanisms for downregulation of I_{to} in HF are still not fully elucidated. In both short-term canine tachypacing models and limited human HF studies, reductions in Kv4.3 protein have been reported (Akar et al. 2005; Zicha et al. 2004). The relatively consistent finding of reduced Kv4.3 mRNA in canine HF models is a plausible mechanism for decreased I_{to} (Akar et al. 2005; Zicha et al. 2004; Kaab et al. 1998). However, gene expression studies in human HF are conflicting, demonstrating decreases (Borlak and Thum 2003) or increases (Soltysinska et al. 2009) in Kv4.3 mRNA. Here, we report an increase in Kv4.3 mRNA at 4 M HF with no change in its protein expression. Consistent with our findings, other animal models of tachypacing-induced HF have reported no change in total Kv4.3 mRNA or protein, yet have also found reduced I_{to} (Rose et al. 2005). One potential

explanation for the reduced current could be a change in the accessory subunit, KChIP2. However, we found no change in KChIP2 protein expression despite a significant increase in KChIP2 mRNA at 4 M HF. This finding is contradictory to reports of KChIP2 mRNA being downregulated in failing human hearts (Radicke et al. 2006; Soltysinska et al. 2009)

Interestingly, we report a prolonged time of I_{to} recovery from inactivation in 4 M HF compared to controls. Such results were not seen in other canine HF studies using midmyocardial cells (Kaab et al., 1996), but were reported in epicardial cells (Cordeiro et al., 2012). DPP6, an ancillary subunit of Kv4.3, has been shown to slow recovery from inactivation in CHO cells when expressed with Kv4.3 (Radicke et al. 2005). Here, we report that gene expression of DPP6 is increased in 4 M HF. More studies will be needed to determine the precise role of DPP6 in modulating cardiac I_{to} , as well as whether I_{to} inactivation contributes to APD₉₀ prolongation at faster heart rates (cycle length < 500 ms) due to the slow recovery from inactivation.

Outward I_{K1} is a modulator of terminal repolarization (Lopatin and Nichols 2001). We observed unchanged inward current with a decrease in the peak outward current (-60 mV) reflecting altered I_{K1} rectification (Lopatin et al. 2000; Carnes and Dech 2002). Because rectification factors, such as polyamines and intracellular magnesium, are involved in the normal gating of I_{K1} (Lopatin et al. 1994), our data suggests a possible role for these factors in decreasing the outward portion of this current in HF. Given the role of I_{K1} in the pathogenesis of arrhythmias (Dhamoon and Jalife 2005), additional study of I_{K1} in HF will be required to clarify the variable results.

The delayed rectifier currents, I_{Kr} and I_{Ks} , play a prominent role in phase 2 and phase 3 repolarization (Nerbonne and Kass 2005). Studies in both humans and canines have suggested that I_{Ks} reduction only prolongs the APD in the setting of downregulation of other K^+ currents (reduced repolarization reserve) (Jost et al. 2013; Roden 1998; Varro et al. 2000). Consistent with a previous 4 to 6 week canine model of HF (Li et al. 2002), we found a reduction in I_{Ks} at 4 M HF. I_{Kr} is a dominant modulator of ventricular repolarization, with reductions evident as both AP and QT prolongation (Tseng 2001). We found a reduction in I_{Kr} in 4 M HF, which does not occur in 4–6 week tachypacing models (Li et al. 2002) or in 1 month HF in the present study. The HF duration-dependent reduction may be explained by hypertrophic modulation of I_{Kr} as this was only observed in the 4 M HF group. This is consistent with reduced I_{Kr} observed in a proarrhythmic chronic AV nodal block canine model of biventricular hypertrophy (Volders et al. 1999). While not measuring I_{Kr} directly, human studies using E-4031 (a specific I_{Kr} blocker) have demonstrated reduced response to I_{Kr} blockade in failing human hearts compared to controls. This study also found Kv11.1 hERG 1a protein expression was reduced compared to controls (Holzem KM et al. 2011), suggesting reduced functional expression of I_{Kr} may be one mechanism contributing to HF-induced I_{Kr} downregulation.

Since we found reductions in multiple repolarizing currents, this suggests a role for reduced repolarization reserve (Roden 1998) as the basis of EAD formation. Reduction of I_{Kr} , specifically, has been demonstrated to produce repolarization instability, which in itself can predict proarrhythmia (Thomsen et al. 2006). Our study showed that chronic HF results in

both AP and QTc prolongation with concurrent increased beat-to-beat variability of cellular repolarization and the appearance of EADs. In normal canine ventricle, combined inhibition of I_{Kr} , I_{Ks} , and I_{to} block can induce EADs (Virag et al. 2011), suggesting these reductions as a mechanism for our observed EADs in HF.

A recent report suggests a role for reactive oxygen species (ROS) in the regulation of I_{Kr} function (Shu et al., 2013). Increased oxidative stress has been implicated in the pathophysiology of several forms of HF, included non-ischemic dilated cardiomyopathy (Sam et al. 2005). While we found no increases in superoxide anion formation, we had previously demonstrated a generalized increase in ventricular ROS in this 4 M HF model (Terentyev et al. 2008). Nitric oxide synthase-dependent ROS are suggested to have a role in the regulation of several repolarizing K^+ currents (Bonilla et al. 2012). In this study, we found increases in Fe-S signal intensity in both 1 M HF and 4 M HF, consistent with increased reduction of these centers that could arise secondary to an increase in nitric oxide (NO) that can block distal electron transport (Zweier et al. 1995; Cleeter et al. 1994). NO has been found to reduce I_{to} in human cardiomyocytes (Gomez et al. 2008) and therefore the observed HF-induced current decreases may be in part attributable to altered NO signaling.

Limitations

Our model is a model of non-ischemic dilated cardiomyopathy, and does not necessarily reflect all etiologies of HF. We also limited our study to ventricular myocytes from the midmyocardial layer which may not fully reflect all transmural changes. We did not assess *in vivo* arrhythmias, but have previously reported increased premature ventricular contractions in chronic canine HF (Kubalova et al. 2005). The present study did not evaluate the contribution of other arrhythmogenic mechanisms; previous work in this model has shown that changes in calcium handling attributable in part to posttranslational modifications of ryanodine receptors by ROS occur (Terentyev et al. 2008) and may also contribute to arrhythmogenesis. Our study also did not evaluate other potentially affected ion currents (e.g. late sodium or sodium-calcium exchanger) which may also contribute to arrhythmogenesis (Valdivia et al. 2005; Sipido et al. 2007).

We did not assess protein expression of all K^+ subunits. Furthermore, differences in mRNA expression also exist between this model and previous reports (Akar et al. 2005; Zicha et al. 2004). The literature on ion channel gene and protein expression in heart failure is highly variable and sometimes contradictory (Nattel et al. 2007; Soltysinska et al. 2009). The variability may reflect the complexity of the system which is affected by modulation downstream of mRNA transcription, such as micro-RNA targeted degradation, post-translational modifications, and/or changes in protein trafficking can determine ion channel function. Therefore, alterations in gene expression may be dynamic and not always translate to equivalent protein expression.

Conclusion

Electrophysiological modeling during human HF is poorly defined due to the reliance on end-stage HF (explanted hearts from transplant recipients) who are treated with multiple drugs which can elicit their own electrophysiologic effects (Haverkamp et al. 2000) and

limited access to true normal controls (Hearse and Sutherland 2000). In this paper, we present a chronic canine HF model which emulates many of the alterations seen in human HF more accurately than other short-term canine tachypacing models. The downregulation of I_{K_r} , not seen in other pacing models, along with other K^+ currents provides a rational mechanism for EAD formation. We present data suggesting that duration of HF produces progressive electrical remodeling, resulting in proarrhythmic potential at the cellular and organ level. Further studies are warranted to elucidate the relationships between ion channel subunit gene, protein and function during heart failure.

Acknowledgments

The authors thank Jeanne Green, RVT for technical assistance and Vadim V. Fedorov, PhD for helpful discussion of the manuscript. Pacing devices and leads provided as a gift of St. Jude Medical.

Grants:

This work was supported by the National Institutes of Health [HL115580, HL089836 to CAC; HL074045 to SG; HL084583, HL083422 to PJM; HL63744, HL65608, HL38324 to JLZ; CA178443 to NL]

Reference List

- Go AS, Mozaffarian D, Roger VL, Benjamin EJ, Berry JD, Blaha MJ, et al. Heart disease and stroke statistics—2014 update: a report from the American Heart Association. *Circulation*. 2014 Jan 21; 129(3):e28–e292. [PubMed: 24352519]
- Tomaselli GF, Zipes DP. What causes sudden death in heart failure? *Circ Res*. 2004 Oct 15; 95(8): 754–63. [PubMed: 15486322]
- Thom T, Haase N, Rosamond W, Howard VJ, Rumsfeld J, Manolio T, et al. Heart disease and stroke statistics—2006 update: a report from the American Heart Association Statistics Committee and Stroke Statistics Subcommittee. *Circulation*. 2006 Feb 14; 113(6):e85–151. [PubMed: 16407573]
- Cohn JN, Ferrari R, Sharpe N. Cardiac remodeling—concepts and clinical implications: a consensus paper from an international forum on cardiac remodeling. Behalf of an International Forum on Cardiac Remodeling. *J Am Coll Cardiol*. 2000 Mar 1; 35(3):569–82. [PubMed: 10716457]
- Hsia HH, Marchlinski FE. Electrophysiology studies in patients with dilated cardiomyopathies. *Card Electrophysiol Rev*. 2002 Dec; 6(4):472–81. [PubMed: 12438831]
- Iles L, Pfluger H, Lefkovits L, Butler MJ, Kistler PM, Kaye DM, et al. Myocardial fibrosis predicts appropriate device therapy in patients with implantable cardioverter-defibrillators for primary prevention of sudden cardiac death. *J Am Coll Cardiol*. 2011 Feb 15; 57(7):821–8. [PubMed: 21310318]
- Haider AW, Larson MG, Benjamin EJ, Levy D. Increased left ventricular mass and hypertrophy are associated with increased risk for sudden death. *J Am Coll Cardiol*. 1998 Nov; 32(5):1454–9. [PubMed: 9809962]
- Beuckelmann DJ, Nabauer M, Kruger C, Erdmann E. Altered diastolic $[Ca^{2+}]_i$ handling in human ventricular myocytes from patients with terminal heart failure. *Am Heart J*. 1995 Apr; 129(4):684–9. [PubMed: 7900618]
- Akar FG, Rosenbaum DS. Transmural electrophysiological heterogeneities underlying arrhythmogenesis in heart failure. *Circ Res*. 2003 Oct 3; 93(7):638–45. [PubMed: 12933704]
- Nishijima Y, Feldman DS, Bonagura JD, Ozkanlar Y, Jenkins PJ, Lacombe VA, et al. Canine nonischemic left ventricular dysfunction: a model of chronic human cardiomyopathy. *J Card Fail*. 2005 Oct; 11(8):638–44. [PubMed: 16230269]
- Sridhar A, Nishijima Y, Terentyev D, Khan M, Terentyeva R, Hamlin RL, et al. Chronic heart failure and the substrate for atrial fibrillation. *Cardiovasc Res*. 2009 Nov 1; 84(2):227–36. [PubMed: 19567484]

- Nishijima Y, Sridhar A, Viatchenko-Karpinski S, Shaw C, Bonagura JD, Abraham WT, et al. Chronic cardiac resynchronization therapy and reverse ventricular remodeling in a model of nonischemic cardiomyopathy. *Life Sci.* 2007 Sep 15; 81(14):1152–9. [PubMed: 17884106]
- Bonilla IM, Sridhar A, Nishijima Y, Gyorke S, Cardounel AJ, Carnes CA. Differential effects of the peroxynitrite donor, SIN-1, on atrial and ventricular myocyte electrophysiology. *J Cardiovasc Pharmacol.* 2013 Jan 29a; 61(5):401–7. [PubMed: 23364607]
- Thomsen MB, Verduyn SC, Stengl M, Beekman JD, de PG, van OJ, et al. Increased short-term variability of repolarization predicts d-sotalol-induced torsades de pointes in dogs. *Circulation.* 2004 Oct 19; 110(16):2453–9. [PubMed: 15477402]
- Sridhar A, Nishijima Y, Terentyev D, Terentyeva R, Uelmen R, Kukielka M, et al. Repolarization abnormalities and afterdepolarizations in a canine model of sudden cardiac death. *Am J Physiol Regul Integr Comp Physiol.* 2008 Nov; 295(5):R1463–R1472. [PubMed: 18768760]
- Bonilla IM, Vargas-Pinto P, Nishijima Y, Pedraza-Toscano A, Ho HT, Long VP III, et al. Ibandronate and Ventricular Arrhythmia Risk. *J Cardiovasc Electrophysiol.* 2013 Nov 20b.
- Nabauer M, Beuckelmann DJ, Erdmann E. Characteristics of transient outward current in human ventricular myocytes from patients with terminal heart failure. *Circ Res.* 1993 Aug; 73(2):386–94. [PubMed: 8330381]
- Carnes CA, Dech SJ. Effects of dihydrotestosterone on cardiac inward rectifier K(+) current. *Int J Androl.* 2002 Aug; 25(4):210–4. [PubMed: 12121570]
- Lopatin AN, Shantz LM, Mackintosh CA, Nichols CG, Pegg AE. Modulation of potassium channels in the hearts of transgenic and mutant mice with altered polyamine biosynthesis. *J Mol Cell Cardiol.* 2000 Nov; 32(11):2007–24. [PubMed: 11040105]
- Livak KJ, Schmittgen TD. Analysis of relative gene expression data using real-time quantitative PCR and the 2(-Delta Delta C(T)) Method. *Methods.* 2001 Dec; 25(4):402–8. [PubMed: 11846609]
- Kumar S, Pan CC, Bloodworth JC, Nixon A, Theuer C, Hoyt DG, et al. Antibody-directed coupling of endoglin and MMP-14 is a key mechanism for endoglin shedding and deregulation of TGF-beta signaling. *Oncogene.* 2013 Sep 30.
- Nishijima Y, Sridhar A, Bonilla I, Velayutham M, Khan M, Terentyeva R, et al. Tetrahydrobiopterin depletion and NOS2 uncoupling contribute to heart failure-induced alterations in atrial electrophysiology. *Cardiovasc Res.* 2011 Jul 1; 91(1):71–9. [PubMed: 21460065]
- Zweier JL, Kuppusamy P, Williams R, Rayburn BK, Smith D, Weisfeldt ML, et al. Measurement and characterization of postschismic free radical generation in the isolated perfused heart. *J Biol Chem.* 1989 Nov 15; 264(32):18890–5. [PubMed: 2553726]
- Zweier JL, Flaherty JT, Weisfeldt ML. Direct measurement of free radical generation following reperfusion of ischemic myocardium. *Proc Natl Acad Sci U S A.* 1987 Mar; 84(5):1404–7. [PubMed: 3029779]
- Zweier JL, Wang P, Kuppusamy P. Direct measurement of nitric oxide generation in the ischemic heart using electron paramagnetic resonance spectroscopy. *J Biol Chem.* 1995 Jan 6; 270(1):304–7. [PubMed: 7814391]
- Oosterhoff P, Oros A, Vos MA. Beat-to-beat variability of repolarization: a new parameter to determine arrhythmic risk of an individual or identify proarrhythmic drugs. *Anadolu Kardiyol Derg.* 2007 Jul; 7(Suppl 1):73–8. [PubMed: 17584687]
- Akar FG, Wu RC, Deschenes I, Armoundas AA, Piacentino V III, Houser SR, et al. Phenotypic differences in transient outward K⁺ current of human and canine ventricular myocytes: insights into molecular composition of ventricular Ito. *Am J Physiol Heart Circ Physiol.* 2004 Feb; 286(2):H602–H609. [PubMed: 14527940]
- Deschenes I, DiSilvestre D, Juang GJ, Wu RC, An WF, Tomaselli GF. Regulation of Kv4.3 current by KChIP2 splice variants: a component of native cardiac I(to)? *Circulation.* 2002 Jul 23; 106(4):423–9. [PubMed: 12135940]
- Radicke S, Cotella D, Graf EM, Ravens U, Wettwer E. Expression and function of dipeptidyl-aminopeptidase-like protein 6 as a putative beta-subunit of human cardiac transient outward current encoded by Kv4.3. *J Physiol.* 2005 Jun 15; 565(Pt 3):751–6. [PubMed: 15890703]

- Houser SR, Margulies KB, Murphy AM, Spinale FG, Francis GS, Prabhu SD, et al. Animal models of heart failure: a scientific statement from the American Heart Association. *Circ Res*. 2012 Jun 22; 111(1):131–50. [PubMed: 22595296]
- Burashnikov A, Di Diego JM, Sicouri S, Doss MX, Sachinidis A, Barajas-Martinez H, et al. A temporal window of vulnerability for development of atrial fibrillation with advancing heart failure. *Eur J Heart Fail*. 2014 Mar; 16(3):271–80. [PubMed: 24464846]
- Akar FG, Spragg DD, Tunin RS, Kass DA, Tomaselli GF. Mechanisms underlying conduction slowing and arrhythmogenesis in nonischemic dilated cardiomyopathy. *Circ Res*. 2004 Oct 1b; 95(7):717–25. [PubMed: 15345654]
- Hanna N, Cardin S, Leung TK, Nattel S. Differences in atrial versus ventricular remodeling in dogs with ventricular tachypacing-induced congestive heart failure. *Cardiovasc Res*. 2004 Aug 1; 63(2): 236–44. [PubMed: 15249181]
- Weber KT, Janicki JS, Shroff SG, Pick R, Chen RM, Bashey RI. Collagen remodeling of the pressure-overloaded, hypertrophied nonhuman primate myocardium. *Circ Res*. 1988 Apr; 62(4):757–65. [PubMed: 2964945]
- Beuckelmann DJ, Nabauer M, Erdmann E. Alterations of K⁺ currents in isolated human ventricular myocytes from patients with terminal heart failure. *Circ Res*. 1993 Aug; 73(2):379–85. [PubMed: 8330380]
- Li GR, Lau CP, Ducharme A, Tardif JC, Nattel S. Transmural action potential and ionic current remodeling in ventricles of failing canine hearts. *Am J Physiol Heart Circ Physiol*. 2002 Sep; 283(3):H1031–H1041. [PubMed: 12181133]
- Sah R, Ramirez RJ, Backx PH. Modulation of Ca²⁺ release in cardiac myocytes by changes in repolarization rate: role of phase-1 action potential repolarization in excitation-contraction coupling. *Circ Res*. 2002 Feb 8; 90(2):165–73. [PubMed: 11834709]
- Akar FG, Wu RC, Juang GJ, Tian Y, Burysek M, Disilvestre D, et al. Molecular mechanisms underlying K⁺ current downregulation in canine tachycardia-induced heart failure. *Am J Physiol Heart Circ Physiol*. 2005 Jun; 288(6):H2887–H2896. [PubMed: 15681701]
- Zicha S, Xiao L, Stafford S, Cha TJ, Han W, Varro A, et al. Transmural expression of transient outward potassium current subunits in normal and failing canine and human hearts. *J Physiol*. 2004 Dec 15; 561(Pt 3):735–48. [PubMed: 15498806]
- Kaas S, Dixon J, Duc J, Ashen D, Nabauer M, Beuckelmann DJ, et al. Molecular basis of transient outward potassium current downregulation in human heart failure: a decrease in Kv4.3 mRNA correlates with a reduction in current density. *Circulation*. 1998 Oct 6; 98(14):1383–93. [PubMed: 9760292]
- Borlak J, Thum T. Hallmarks of ion channel gene expression in end-stage heart failure. *FASEB J*. 2003 Sep; 17(12):1592–608. [PubMed: 12958166]
- Soltysinska E, Olesen SP, Christ T, Wettwer E, Varro A, Grunnet M, et al. Transmural expression of ion channels and transporters in human nondiseased and end-stage failing hearts. *Pflugers Arch*. 2009 Nov; 459(1):11–23. [PubMed: 19768467]
- Rose J, Armondas AA, Tian Y, DiSilvestre D, Burysek M, Halperin V, et al. Molecular correlates of altered expression of potassium currents in failing rabbit myocardium. *Am J Physiol Heart Circ Physiol*. 2005 May; 288(5):H2077–H2087. [PubMed: 15637125]
- Radicke S, Cotella D, Graf EM, Banse U, Jost N, Varro A, et al. Functional modulation of the transient outward current I_{to} by KCNE beta-subunits and regional distribution in human non-failing and failing hearts. *Cardiovasc Res*. 2006 Sep 1; 71(4):695–703. [PubMed: 16876774]
- Lopatin AN, Nichols CG. Inward rectifiers in the heart: an update on I(K1). *J Mol Cell Cardiol*. 2001 Apr; 33(4):625–38. [PubMed: 11273717]
- Lopatin AN, Makhina EN, Nichols CG. Potassium channel block by cytoplasmic polyamines as the mechanism of intrinsic rectification. *Nature*. 1994 Nov 24; 372(6504):366–9. [PubMed: 7969496]
- Dhamoon AS, Jalife J. The inward rectifier current (IK1) controls cardiac excitability and is involved in arrhythmogenesis. *Heart Rhythm*. 2005 Mar; 2(3):316–24. [PubMed: 15851327]
- Nerbonne JM, Kass RS. Molecular physiology of cardiac repolarization. *Physiol Rev*. 2005 Oct; 85(4): 1205–53. [PubMed: 16183911]

- Jost N, Virag L, Comtois P, Ordog B, Szuts V, Seprenyi G, et al. Ionic mechanisms limiting cardiac repolarization reserve in humans compared to dogs. *J Physiol*. 2013 Sep 1; 591(Pt 17):4189–206. [PubMed: 23878377]
- Roden DM. Taking the “idio” out of “idiosyncratic”: predicting torsades de pointes. *Pacing Clin Electrophysiol*. 1998 May; 21(5):1029–34. [PubMed: 9604234]
- Varro A, Balati B, Iost N, Takacs J, Virag L, Lathrop DA, et al. The role of the delayed rectifier component IKs in dog ventricular muscle and Purkinje fibre repolarization. *J Physiol*. 2000 Feb 15; 523(Pt 1):67–81. [PubMed: 10675203]
- Tseng GN. I(Kr): the hERG channel. *J Mol Cell Cardiol*. 2001 May; 33(5):835–49. [PubMed: 11343409]
- Volders PG, Sipido KR, Vos MA, Spatjens RL, Leunissen JD, Carmeliet E, et al. Downregulation of delayed rectifier K(+) currents in dogs with chronic complete atrioventricular block and acquired torsades de pointes. *Circulation*. 1999 Dec 14; 100(24):2455–61. [PubMed: 10595960]
- Holzem KM, Glukhov AV, Efimov IR. The role of IKr in transmural repolarization abnormalities in human heart failure. *Circulation*. 2011; 124 Ref Type: Generic.
- Thomsen MB, Volders PG, Beekman JD, Matz J, Vos MA. Beat-to-Beat variability of repolarization determines proarrhythmic outcome in dogs susceptible to drug-induced torsades de pointes. *J Am Coll Cardiol*. 2006 Sep 19; 48(6):1268–76. [PubMed: 16979017]
- Sam F, Kerstetter DL, Pimental DR, Mulukutla S, Tabaei A, Bristow MR, et al. Increased reactive oxygen species production and functional alterations in antioxidant enzymes in human failing myocardium. *J Card Fail*. 2005 Aug; 11(6):473–80. [PubMed: 16105639]
- Terentyev D, Gyorke I, Belevych AE, Terentyeva R, Sridhar A, Nishijima Y, et al. Redox modification of ryanodine receptors contributes to sarcoplasmic reticulum Ca²⁺ leak in chronic heart failure. *Circ Res*. 2008 Dec 5; 103(12):1466–72. [PubMed: 19008475]
- Bonilla IM, Sridhar A, Gyorke S, Cardounel AJ, Carnes CA. Nitric oxide synthases and atrial fibrillation. *Front Physiol*. 2012; 3:105. [PubMed: 22536189]
- Cleeter MW, Cooper JM, Darley-Usmar VM, Moncada S, Schapira AH. Reversible inhibition of cytochrome c oxidase, the terminal enzyme of the mitochondrial respiratory chain, by nitric oxide. Implications for neurodegenerative diseases. *FEBS Lett*. 1994 May 23; 345(1):50–4. [PubMed: 8194600]
- Gomez R, Nunez L, Vaquero M, Amoros I, Barana A, de PT, et al. Nitric oxide inhibits Kv4.3 and human cardiac transient outward potassium current (Ito1). *Cardiovasc Res*. 2008 Dec 1; 80(3):375–84. [PubMed: 18678642]
- Kubalova Z, Terentyev D, Viatchenko-Karpinski S, Nishijima Y, Gyorke I, Terentyeva R, et al. Abnormal intrastore calcium signaling in chronic heart failure. *Proc Natl Acad Sci U S A*. 2005 Sep 27; 102(39):14104–9. [PubMed: 16172392]
- Valdivia CR, Chu WW, Pu J, Foell JD, Haworth RA, Wolff MR, et al. Increased late sodium current in myocytes from a canine heart failure model and from failing human heart. *J Mol Cell Cardiol*. 2005 Mar; 38(3):475–83. [PubMed: 15733907]
- Sipido KR, Bito V, Antoons G, Volders PG, Vos MA. Na/Ca exchange and cardiac ventricular arrhythmias. *Ann N Y Acad Sci*. 2007 Mar. 1099:339–48. [PubMed: 17446474]
- Nattel S, Maguy A, Le BS, Yeh YH. Arrhythmogenic ion-channel remodeling in the heart: heart failure, myocardial infarction, and atrial fibrillation. *Physiol Rev*. 2007 Apr; 87(2):425–56. [PubMed: 17429037]
- Haverkamp W, Breithardt G, Camm AJ, Janse MJ, Rosen MR, Antzelevitch C, et al. The potential for QT prolongation and pro-arrhythmia by non-anti-arrhythmic drugs: clinical and regulatory implications. Report on a Policy Conference of the European Society of Cardiology. *Cardiovasc Res*. 2000 Aug; 47(2):219–33. [PubMed: 10947683]
- Hearse DJ, Sutherland FJ. Experimental models for the study of cardiovascular function and disease. *Pharmacol Res*. 2000 Jun; 41(6):597–603. [PubMed: 10816328]

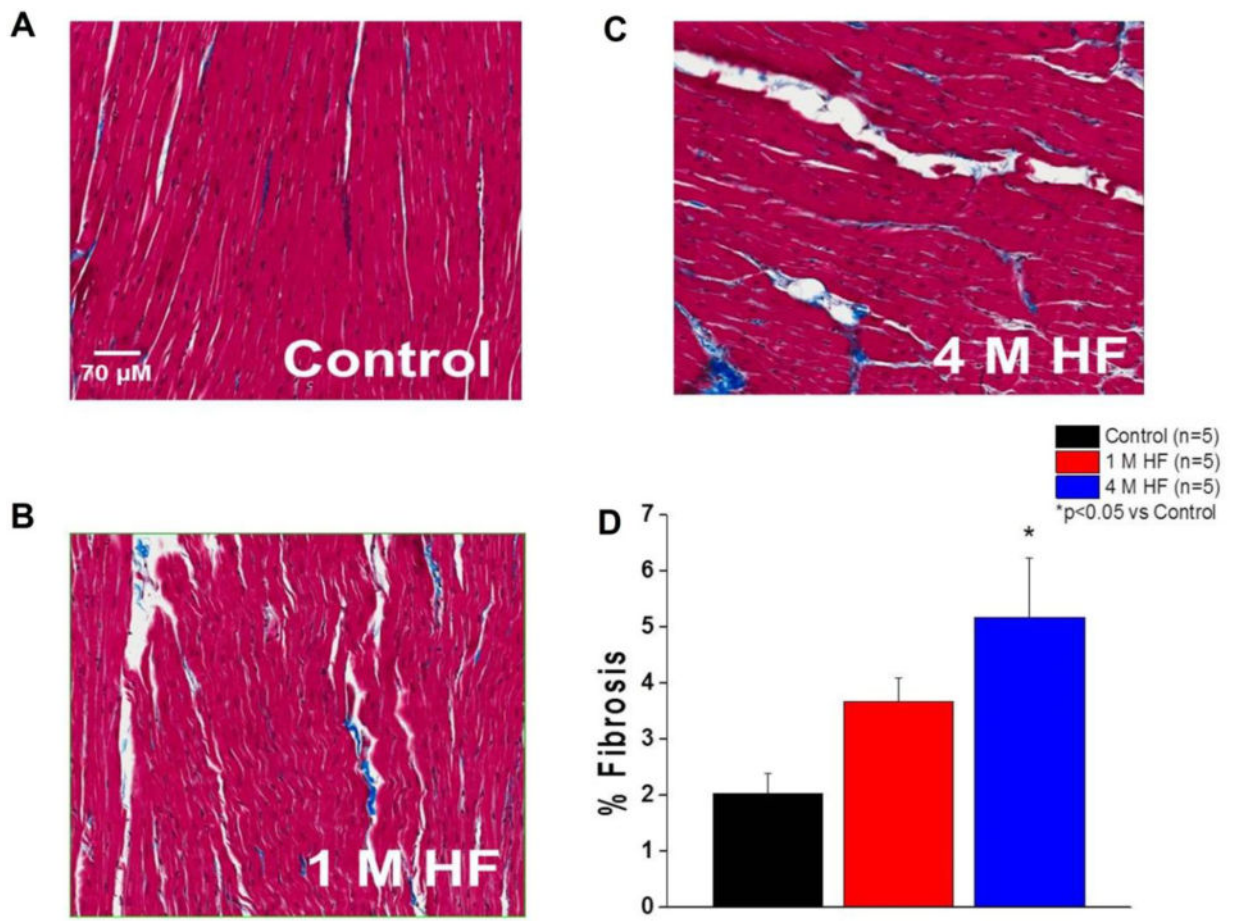


Figure 1. Interstitial Fibrosis is Increased in Chronic HF

Representative Masson's Trichrome staining of LV tissue. **A.** Control. **B.** 1 M HF. **C.** 4 M HF. **D.** Summary data (* $p < 0.05$ vs control).

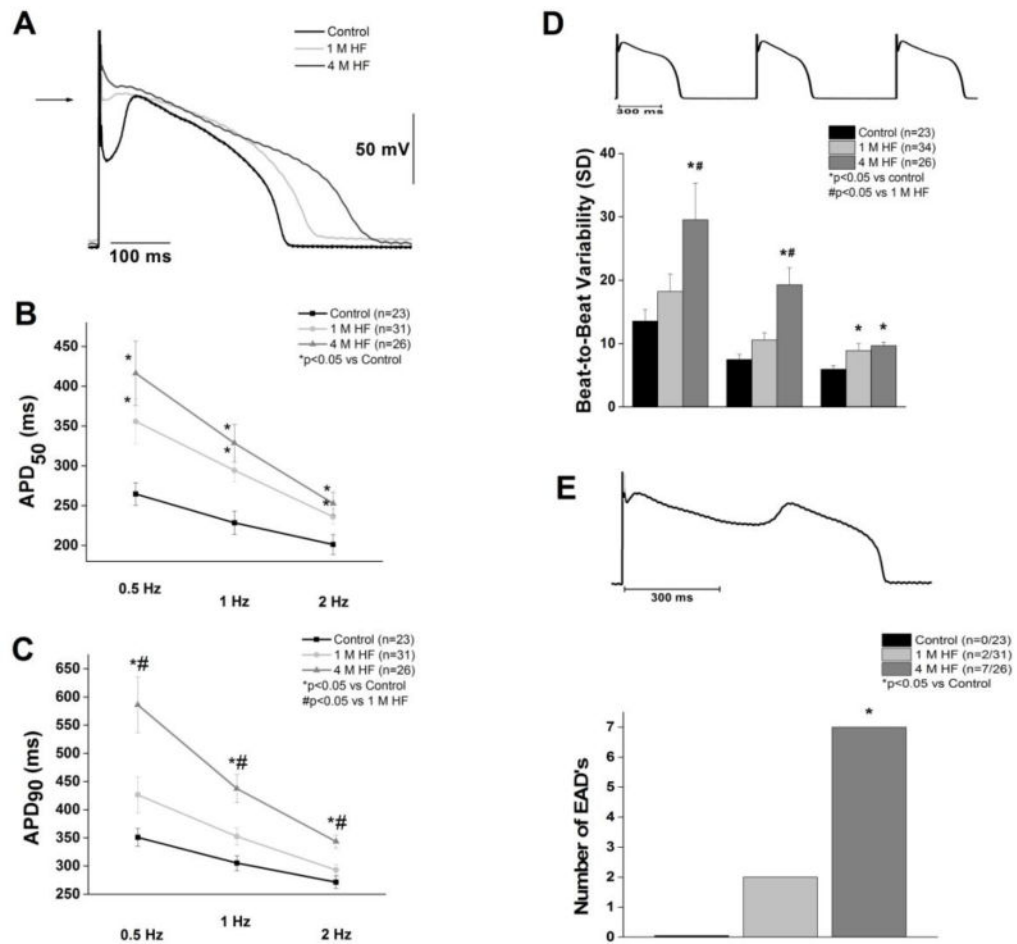


Figure 2. Progressive action potential prolongation and cellular arrhythmias during heart failure
A. Representative action potentials at 1 Hz. **B.** APD₅₀ is prolonged at 1 and 4 months of HF ($p < 0.05$). **C.** APD₉₀ is significantly prolonged in 4 M HF compared to 1 M HF and control ($p < 0.05$). **D.** Beat-to-beat variability (representative, top) was significantly increased in 4 M HF ($*p < 0.05$ vs. control, $\#p < 0.05$ vs. 1M HF). **E.** Early afterdepolarizations (representative, top) were more frequent in 4 M HF ($*p < 0.05$ vs control).

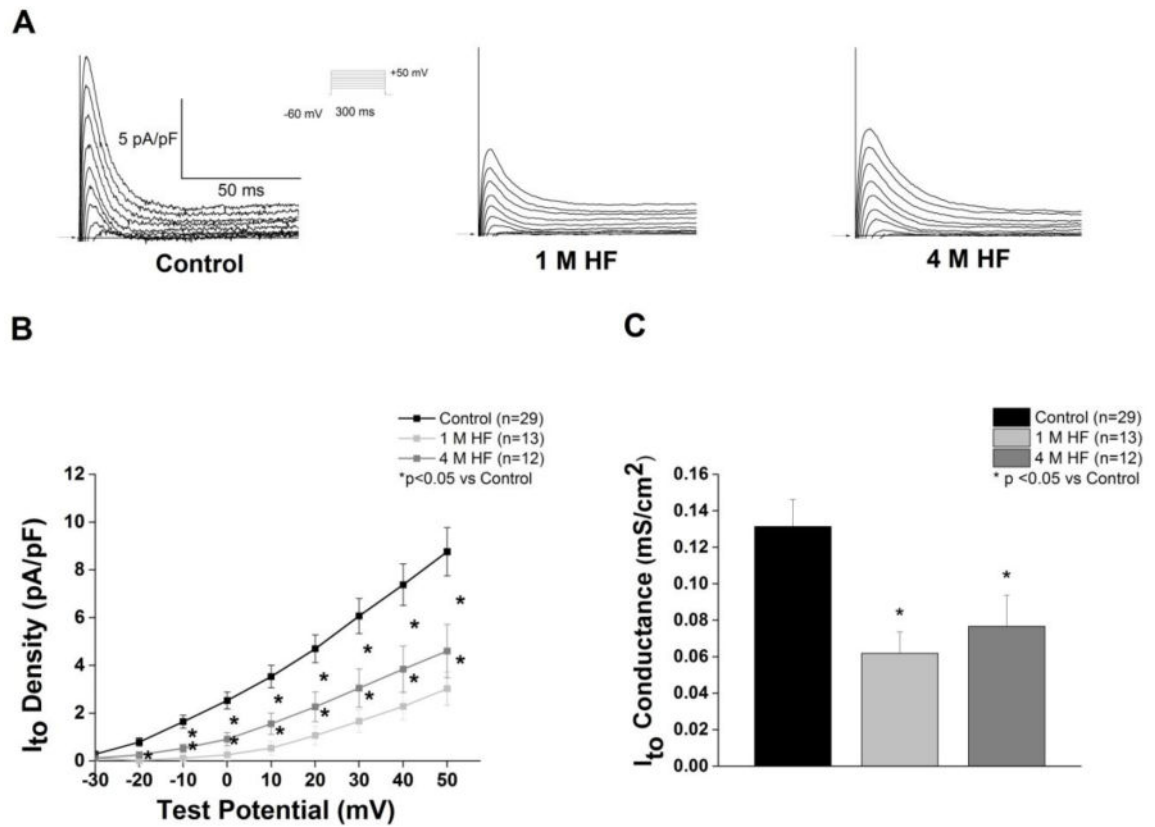


Figure 3. HF decreases I_{to}

A. Representative I_{to} current tracings from each group; voltage protocol shown in the inset.

B. I–V curves (*p<0.05 vs. control) **C.** I_{to} slope conductance is decreased in HF (*p<0.05).

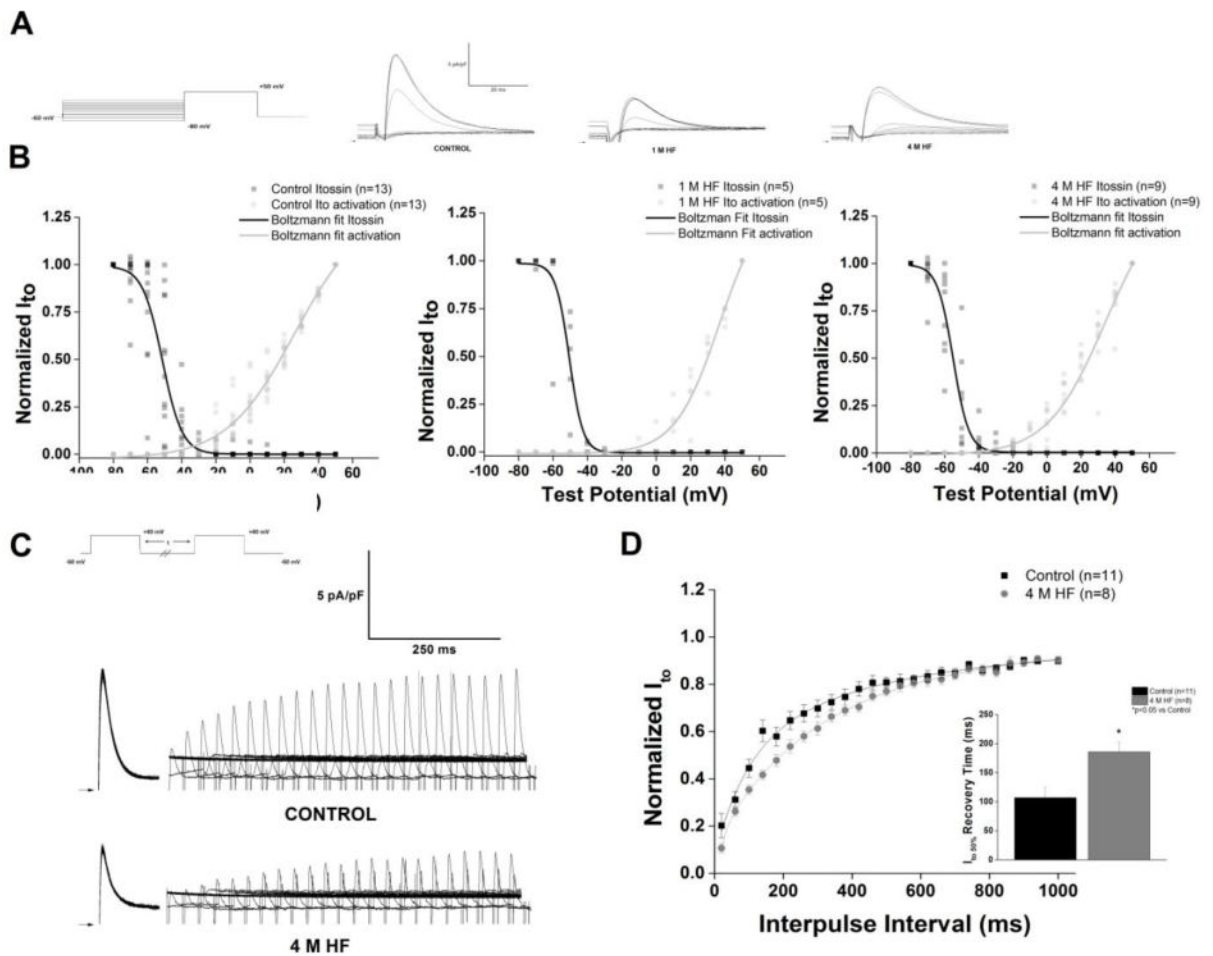


Figure 4. I_{to} kinetics are altered in chronic HF

A. Representative steady state inactivation traces of I_{to} recorded with the voltage protocol displayed in the inset. **B.** Steady state inactivation and activation curves of I_{to} fit to Boltzmann functions, demonstrates a “window” current, that is reduced as the heart fails. **C.** Representative traces elicited by two-step protocol in control and 4 M HF; voltage protocol in inset. **D.** Summary data of recovery from inactivation; HF significantly prolongs recovery to 50% of total I_{to} current ($p < 0.05$ vs control).

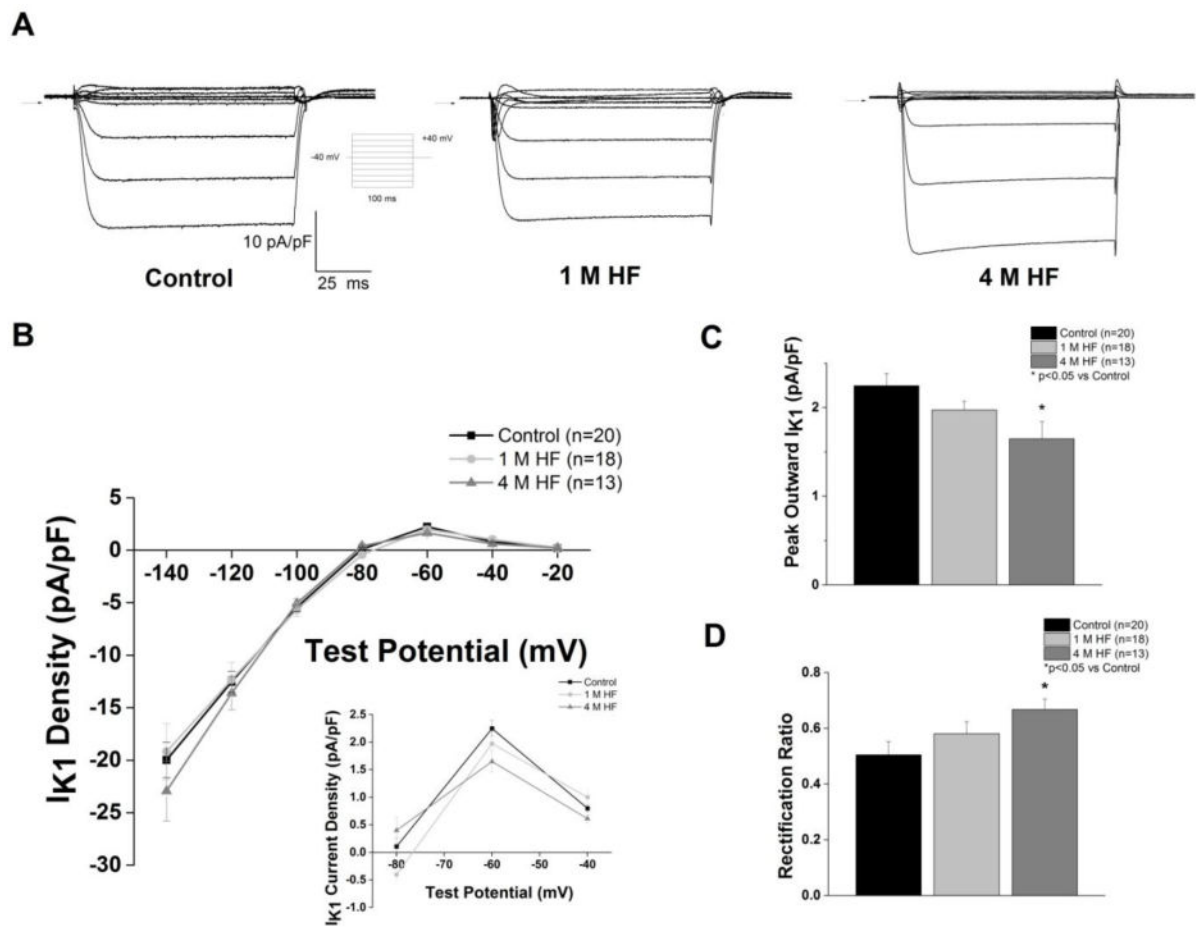


Figure 5. Outward I_{K1} , but not inward I_{K1} , is reduced in chronic but not short-term HF
A. Representative I_{K1} current tracing, voltage protocol displayed in the inset. **B.** I–V curves; inset shows expanded I–V curve of outward I_{K1} . **C.** Peak outward I_{K1} is significantly reduced in 4 M HF vs. control ($p<0.05$). **D.** Rectification ratio is significantly increased in 4 M HF vs control ($p<0.05$).

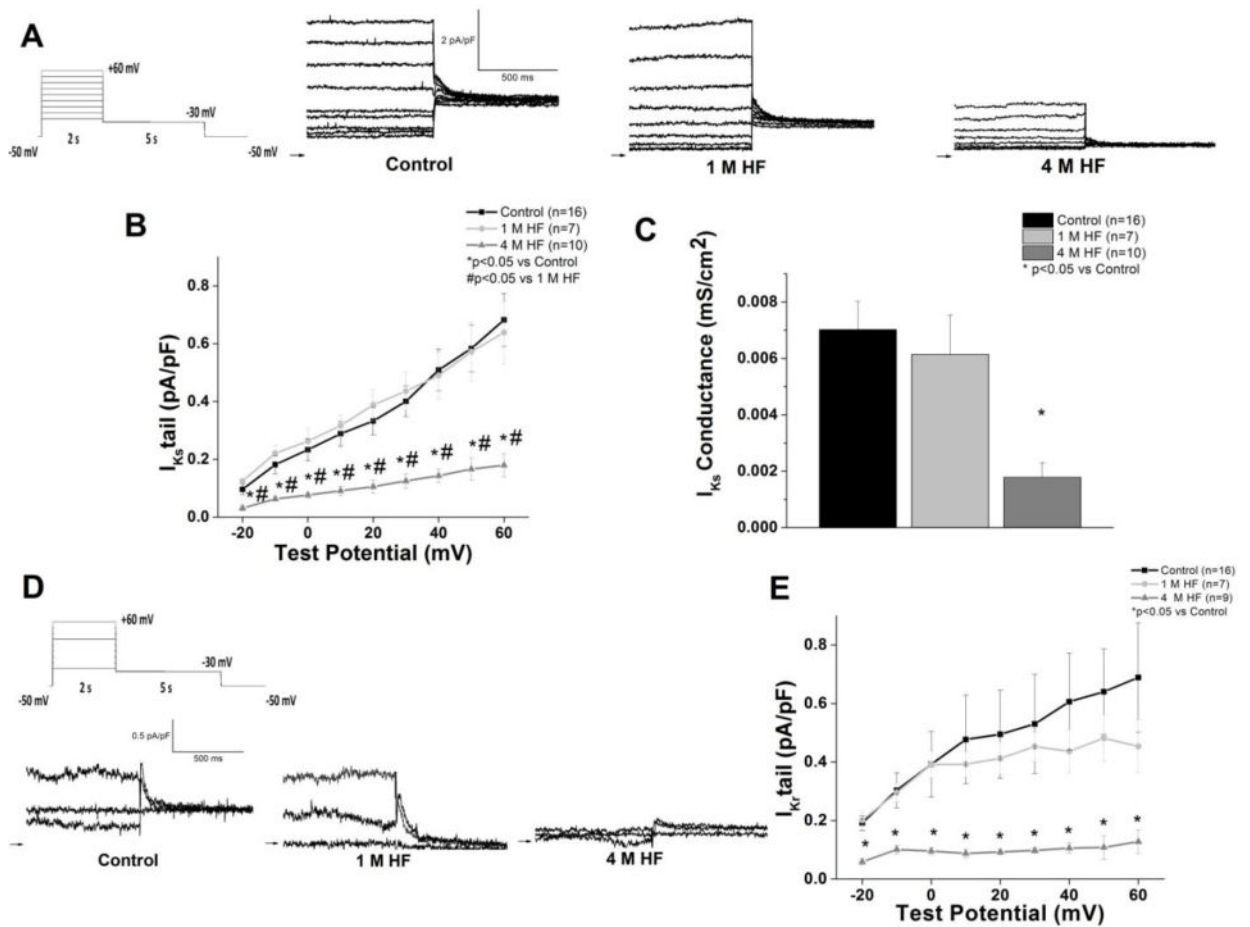


Figure 6. I_{Ks} and I_{Kr} are reduced in chronic HF

A. Representative I_{Ks} tail currents (defined as the sotalol-insensitive current) from each group; inset: voltage protocol **B.** I–V curves (* $p < 0.05$ vs. control; # $p < 0.05$ vs. 1 M HF) **C.** I_{Ks} slope conductance is reduced in 4 M HF ($p < 0.05$ vs control). **D.** Representative I_{Kr} tail currents (defined as the sotalol-sensitive current) recorded with the same voltage protocol in (A). For ease of viewing, only traces recorded -20 mV, $+30$ mV, and $+60$ mV are depicted. **E.** I_{Kr} I–V curves (* $p < 0.05$ vs control).

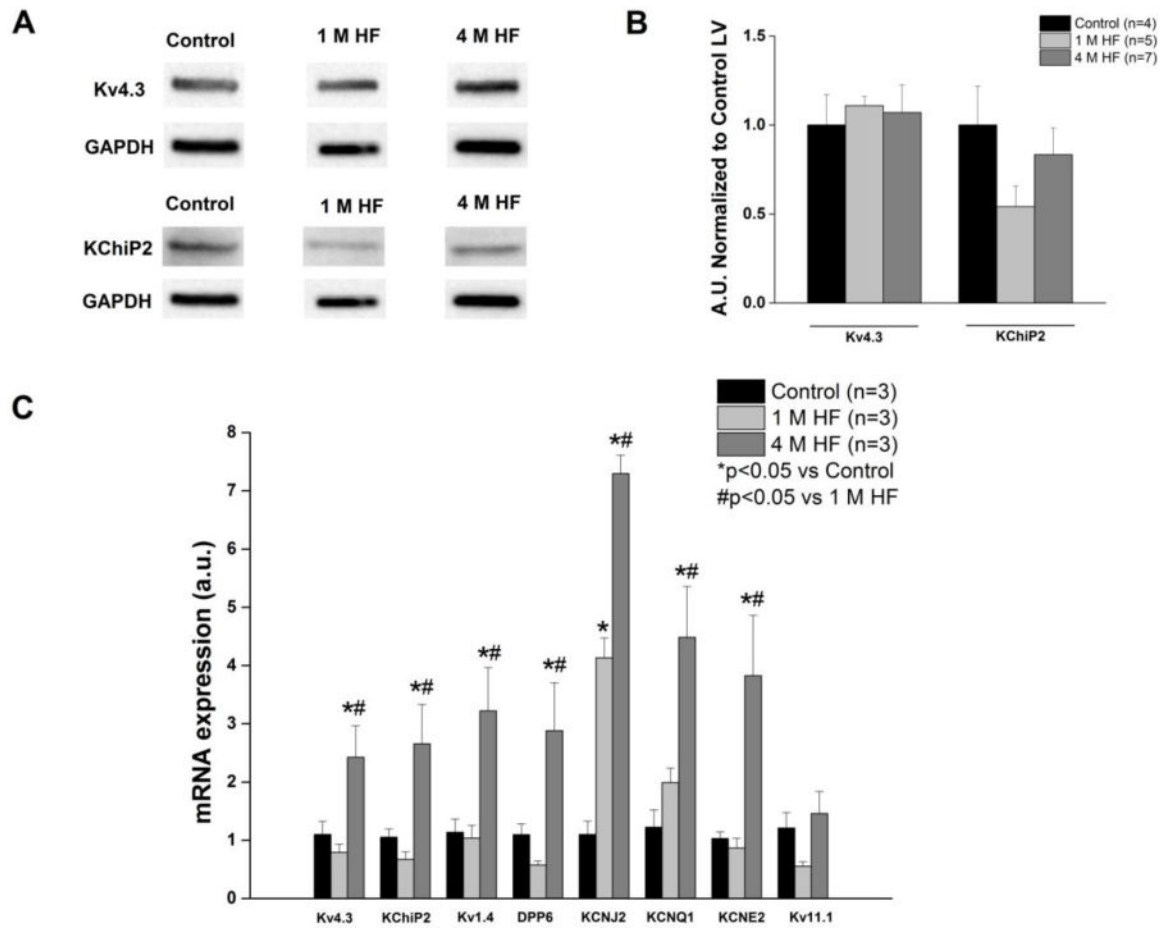


Figure 7. Protein expression and mRNA levels of K⁺ channel subunits

A. Representative Western Blots of I_{to} subunits Kv4.3 and KChIP2. **B.** Summary data of Kv4.3 and KChIP2 protein expression (p=NS). **C.** mRNA for K⁺ channel subunits. (*p<0.05 vs. control; #p<0.05 vs. 1 M HF).

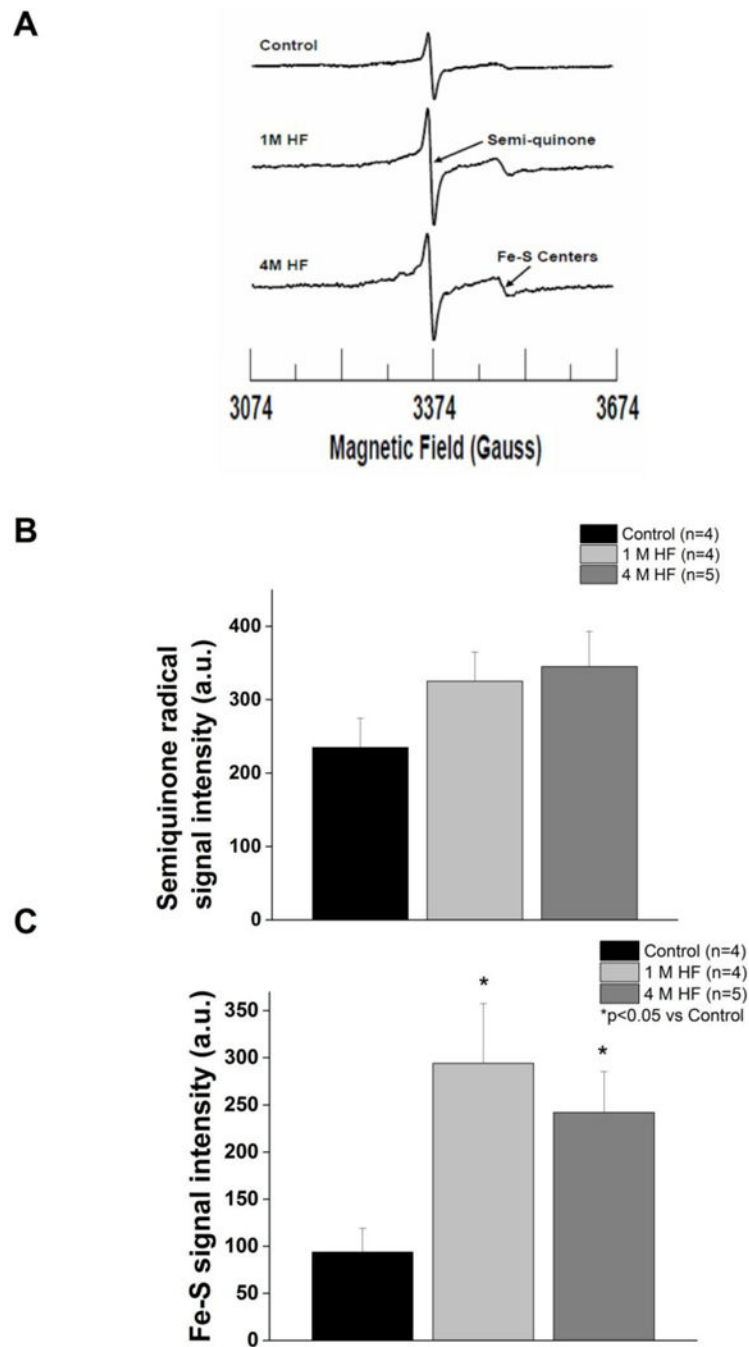


Figure 8. Heart failure increases ventricular oxidative stress

A. Representative EPR spectra of tissue homogenates measured at 77 K in control, 1 M HF, and 4 M HF. B. Summary data of semi-quinone radical centers. (C) Summary data of Fe-S centers. ($p < 0.05$ vs. control).

TABLE 1

Echocardiographic and Electrocardiogram parameters in 4 M HF animals

	Baseline	1 Month HF	4 Month HF
Fractional shortening (%)	29.6 ± 1.49	15.2 ± 0.97*	11.2 ± 0.84*, #
Left Ventricle Dimension (cm)			
Diastole	3.46 ± 0.13	4.33 ± 0.15*	5.28 ± 0.21*, #
Systole	2.41 ± 0.07	3.67 ± 0.12*	4.68 ± 0.18*, #
Left Ventricle mass (g)	91.6 ± 9.15	121.2 ± 11.0	157.7 ± 16.1*, #
ECG parameters			
PR (ms)	110.7 ± 5.24	108.1 ± 5.01	107.9 ± 3.85
QRS (ms)	45.8 ± 2.47	50.1 ± 3.03	54.2 ± 4.10*
RR (ms)	578.4 ± 35.4	520.2 ± 53.3	511.2 ± 69.4
QT (ms)	201.1 ± 6.10	199.6 ± 7.40	198.9 ± 8.38
QT _{cf} (ms)	242.5 ± 3.35	250.1 ± 4.59	252.4 ± 4.33*

N=7–10 per observation;

* p<0.05 vs baseline;

p<0.05 vs 1 M HF. Values are means ± SE.

Author Manuscript

Author Manuscript

Author Manuscript

Author Manuscript